Optimization of 2-DE and multiplexed detection of O-GlcNAcome, phosphoproteome and whole proteome protocol of synapse-associated proteins within the rat sensorimotor cortex

Julie Fourneau, Caroline Cieniewski-Bernard, Marie-Hélène Canu, Sophie
Duban-Deweer, Johann Hachani, Bruno Bastide, Erwan Dupont

Optimization of 2-DE and multiplexed detection of O-GlcNAcome, phosphoproteome and whole proteome protocol of synapse-associated proteins within the rat sensorimotor cortex

Julie Fourneau[1], Caroline Cieniewski-Bernard[1], Marie-Hélène Canu[1], Sophie Duban-Deweer[2], Johann Hachani[2], Bruno Bastide[1] and Erwan Dupont[1]

(1) Univ. Lille, Univ Artois, Univ Littoral Côte d'Opale, ULR7369, URePSSS – Unité de Recherche Pluridisciplinaire Sport Santé Société, F–59000 Lille, France.

(2) Univ. Artois, ULR2465, Laboratoire de la Barrière Hémato-Encéphalique (LBHE), plateau de Spectrométrie de Masse de l'ARTOIS (SMART), F-62300 Lens, France

Correspondence: Marie-Hélène CANU, EURASPORT, 413 Avenue Eugène Avinée, 59120, Loos, France.

E-mail: marie-helene.canu@univ-lille.fr

Type of article: research paper

Abbreviations: ASB-14, amidosulfobetaine; **IAA**, iodoacetamide; **NC**, negative control; **NL**, nonlinear; **OGA**, O-GlcNAcase; **OGT**, O-GlcNAc transferase; **P**, pellet; **PSD**, postsynaptic density; **S**, supernatant; **TGX**, Tris-Glycine; **TBP**, tributylphosphine

Abstract

Background: Several studies have shown the importance of phosphorylation, O-GlcNAcylation and their interplay in neuronal processes.

New Method: To get understanding about molecular mechanisms of synaptic plasticity, we performed a preparation of synaptic protein-enriched fraction on a small sample of rat sensorimotor cortex. We then optimized a multiplexed proteomic strategy to detect O-GlcNAcylated proteins, phosphoproteins, and the whole proteome within the same bidimensional gel. We compared different protocols (solubilisation buffer, reticulation and composition of the gel, migration buffer) to optimize separating conditions for 2D-gel electrophoresis of synaptic proteins. The O-GlcNAcome was revealed using Click chemistry and the azide–alkyne cycloaddition of a fluorophore on O-GlcNAc moieties. The phosphoproteome was detected by Phospho-Tag staining, while the whole proteome was visualized through SYPRORuby staining.

Results: This method permitted, after sequential image acquisition, the direct in-gel detection of O-GlcNAcome, phosphoproteome, and whole proteome of synapse-associated proteins.

Conclusion: This original method of differential proteomic analysis will permit to identify key markers of synaptic plasticity that are O-GlcNAcylated and/or phosphorylated, and their molecular regulations in neuronal processes.

Keywords: 2-DE / O-GlcNAcylation / Phosphorylation / Proteomic / synapse-associated proteins

1. Introduction

Synapses are areas of functional contact between axonal endings of a neuron and other cells at the level of a dendrite, soma or even another axon. Proteomic analysis of synapses has been rarely explored so far, mainly due to difficulties to enrich synaptic proteins and because of low level of protein materials.

The first protein inventory in a mammalian synapse was performed on by proteomic characterization of synaptosomes isolated from mouse brain (Schrimpf et al., 2005) and rat cerebral cortex (Witzmann et al., 2005). Around 1000 proteins were identified by LC-MS/MS in both studies. A thorough analysis has shown that identified proteins are involved in synaptic vesicle trafficking or docking (synaptic vesicle exocytosis and recycling), receptor or transporter functions (such as postsynaptic receptors) and proteins constituting the PSD, a large number of soluble and membrane-bound proteins for synaptic signal transduction that affect synaptic transmission and metabolism (Filiou et al., 2010). Advancement of subcellular compartment fractionation techniques allowed neuroscientists to study more specifically and separately pre- and postsynaptic proteomes. By a combination of modern molecular, biophysical, electron microscopy, and modelling techniques, synaptic vesicles have been specifically studied and 80 components were identified allowing the construction of prototypical molecular model of synaptic vesicle (Volknandt and Karas, 2012). Another example of discovery concerns the PSD, defined as the postsynaptic active zone, which includes more than 1000 different proteins revealing a high degree of molecular complexity (Bayés et al., 2012).

Most studies of the molecular mechanisms of neuroplasticity were focused on a fundamental and omnipresent post-translational modification: the phosphorylation. At the pre- and post-synaptic level, phosphorylation regulates trafficking of proteins involved in the molecular events underlying growth cone migration, synapse formation, neurotransmission, and synaptic plasticity. According to Filiou et al. (Filiou et al., 2010), more than 100 phosphoproteins were identified in rat cortical synaptosomes, supporting a key role of phosphorylation at the nerve terminal. Phosphorylation sites in PSD of synaptosomes were mapped in different mouse brain structures (Filiou et al., 2010), the phosphoproteins involved in adhesion/cytoskeleton representing the most prevalent class, followed by proteins involved in adaptor/sorting functions.

However, phosphorylation is not the only post-translational modification involved in the modulation of these different aspects of cell machinery. The concept of a closely regulated dynamics between phosphorylation and an atypical glycosylation, the O-N-acetyl-β-D-glucosaminylation or O-GlcNAcylation, has emerged over the past two decades. O-GlcNAcylation modifies serine and threonine residues of nuclear, cytoplasmic and mitochondrial proteins, and is involved in various intracellular functions such as gene expression, from transcription to translation, regulation of intracellular signaling or protein turnover (Ma and Hart, 2014). Such as phosphorylation, O-GlcNAcylation is highly dynamic and reversible, regulation of the process being catalyzed by coordinated actions of O-GlcNAc Transferase (OGT) and O-GlcNAcase (OGA). Physiological roles of protein O-GlcNAcylation is particularly important in central nervous system (Ogawa et al., 2015). Indeed, OGT is present in dendrites and axon terminals (Akimoto et al., 2003). Using the approach of Khidekel et al. (Khidekel et al., 2004), 25 proteins were identified from rat forebrain. As expected, these proteins were functionally categorized as proteins associated with gene expression, neuronal signalling, and synaptic plasticity. According to Vosseller et al. (Vosseller et al., 2006), 145 O-GlcNAc modified peptides were identified from a PSD preparation of mouse brain; O-GlcNAc sites were mapped on 65 O-GlcNAcylated peptides, which belong to proteins involved in synapse assembly, synaptic vesicle trafficking, and postsynaptic signalling. Importantly, Khidekel et al. (Khidekel et al., 2007) demonstrated that O-GlcNAcylation is dynamically modulated by excitatory stimulation, suggesting its involvement in synaptic plasticity.

Thus, phosphorylation, O-GlcNAcylation and their interplay may play a key role in molecular processes implicated in synaptic plasticity since over 1 750 O-GlcNAcylated and 16 500 phosphorylated sites have been identified in synapse (Trinidad et al., 2012). However, this interplay remains poorly understood. In this study, we propose to optimize two dimensional electrophoresis methods developed for muscle tissue (Cieniewski-Bernard et al., 2014) in order to evaluate O-GlcNAcylation/phosphorylation interplay on fractions of cerebral cortex enriched in synaptic proteins. A multiplexed proteomic strategy was optimized to detect O-GlcNAcome, phosphoproteome, and the whole proteome within the same gel, to quickly compare these proteomes. Moreover, most proteomic studies have been performed on whole brain, or after pooling brain structures (hippocampus, forebrain, striatum…). We propose herein an optimized and reproducible protocol for the proteomic analysis of small amount of rat cerebral cortex. At terms, this method will improve our knowledge about molecular processes implicated in neuronal modifications and adaptations encountered under normal (adaptation to the environment, ageing...) or pathological (neurodegenerative, neurodevelopmental, trauma...) conditions.

2. Materials and methods

2.1. Animal

The procedure was carried out in accordance with European Communities Council Directive 2010/63/UE, and were approved by Regional Committee on the Ethics of Animal Experiments of Nord Pas-de-Calais region (CEEA 75, reference Number: APAFIS#4733-20 16032917266176 v4). Male Wistar rats (280–320g) were housed under temperature and light controlled conditions (23°C, 12h light/12h dark cycle) and had *ad libitum* access to water and food.

2.2. Tissue sampling

Brain tissue samples were collected under deep anaesthesia (sodium pentobarbital, 60mg/kg, Ceva Animal Health). Firstly, thoracic cavity was open to allow access to the heart. Intracardiac infusion of ice-cold solution of NaCl 0.9% was then performed until total exsanguination of the animal. Then, the head of the animal was fixed in a stereotaxic frame, and a craniotomy was performed to expose cerebral cortex. The dura-mater was resected. A sample of sensorimotor cortex was taken at stereotaxic coordinates anterior 0 to -2 and lateral 2 to 4 on the two hemispheres, corresponding to the hindlimb somatotopic area. Samples were placed in liquid nitrogen and stored at -80°C. Total duration of the sampling did not exceed 10min.

2.3. Enrichment in synaptic proteins

A protocol adapted from Kamat et al. (Kamat et al., 2014) was used to perform enrichment in synaptic proteins of small amounts (~20mg) of sensorimotor cortex (Fig. 1). Brain samples were homogenized using ice-cold HEPES buffer (145mM NaCl, 5mM KCl, 2mM $CaCl_2$, 1mM $MgCl_2$, 5mM glucose, 5mM HEPES, 50µM PUGNAc, anti-proteases (Complete EDTA-free, Roche Diagnostic), anti-phosphatases (Phos-Stop, Roche Diagnostic), pH7.4) containing 0,32M sucrose. Initial homogenate was centrifuged at 600 × g for 10 min at 4°C and supernatant (S1) was then diluted 1:1 with 1.3M sucrose in HEPES buffer, to yield a suspension at a final concentration of 0.8M sucrose in HEPES buffer. This suspension was further centrifuged at 20 000 × g for 30min and supernatant (S2) (cytosol fraction) was collected; the pellet (P2) (containing crude synaptosomes as well as contaminating neuronal, mitochondrial and glial membranes) was washed 2 to 3 times with HEPES buffer and centrifuged at 12 000 × g for 15min. The final pellet (P2') corresponding to the synaptic protein-enriched fraction was resuspended in RIPA buffer to disrupt synaptic membranes (10mM Tris-HCl,

150mM NaCl, 1mM EDTA, 0,2% Triton X-100, 0.5% Na$^+$ deoxycholate, 0.1% SDS, pH7.4, containing anti-proteases, anti-phosphatases and PUGNAc). Protein concentration of the supernatant was determined by a Bradford assay.

2.4. Two-dimensional electrophoresis

Chloroform/methanol precipitation: Briefly, the sample volume was adjusted to 200µl with ultrapure water. Six hundred microliters of methanol were added and sample was vortexed. After addition of chloroform (150µl volume) and a brief vortex, 400µl of water were finally added, and sample was briefly vortexed. After centrifugation at 15 000 × g for 5min, the upper aqueous phase was carefully discarded while the interface layer (corresponded to proteins precipitate) was leaved intact. A volume of 450µl of methanol was added and the sample was vortexed and centrifuged at 15 000 × g for 5min. The supernatant was removed and the pellet was air-dried for 10min.

Isoelectric focusing: After chloroform/methanol precipitation, sample of synapse-associated proteins (50-200µg) was diluted in a solubilisation buffer composed of urea (7M), thiourea (2M), ampholytes (IPG Buffer pH 3-11 NL, 1%, GE Healthcare) and bromophenol blue. Various detergent concentrations (0-4%) or reducing agents (5-60mM) were also added: CHAPS (Sigma-Aldrich) and/or ASB-14 (amino-sulfobetaine-14, Sigma-Aldrich), and DTT (Biorad) and/or TBP (tributylphosphine, Biorad), respectively. The sample was stirred under vigorous agitation at room temperature for 1h. It was then applied on IPG strip (Immobiline® DryStrip, 11cm, pH 3-11, non-linear, GE Healthcare) to ensure sample uptake overnight through passive rehydration (12h). Next day, strip was placed on i12 Focusing Tray (BioRad); once electrodes positioned, strip was covered with mineral oil and the IEF was started at 20°C. The IEF was carried out in several steps using Protean i12 IEF cell system (BioRad): the strip was subjected to 250V for 20min, a gradual increase up to 8000V for one hour, and up to 8000V to reach 26000V/h. Limit of current was set at 50µA and duration of isoelectrofocusing was about 7h.

Equilibrations: The strip was bathed for 10min in an equilibration buffer (6M urea, 2% SDS, 0.375M Tris-HCl, 30% glycerol) also containing 2% DTT and then 10min in equilibration buffer containing 2.5% iodoacetamide (IAA) and bromophenol blue.

SDS-PAGE: The second dimension was carried out on a polyacrylamide gel (BioRad). To optimize separation according to molecular weight of proteins, gels of various degrees of crosslinking (4-20% or 8-16%) and composition (TGX or TGX Stain-Free™ or Tris-HCl) were used (Table 1). Once equilibration achieved, strip was deposited on the surface of separating gel. Electrophoretic separation was carried out in different migration buffers (0.2M trailing ion, pH 8.3, 0.02M Tris-base, 0.2% SDS). Two different trailing ions have been used: glycine or taurine. Migration was performed at constant intensity (25mA per gel) for about 6h, until migration front comes out of the gel. After electrophoretic separation, gel was incubated at least 30min in fixing solution (10% trichloroacetic acid, 50% methanol) and then washed with ultrapure water 3 x 10min under stirring.

Table 1. Protocols tested for IEF and SDS-PAGE optimization of synapse-associated proteins sample.

Protocol		Quantity	Solubilisation buffer	Strip rehydration	Acrylamide gel composition	Migration buffer
1	A	100 µg	5 mM TBP + 2 % CHAPS	Passive 12h	4–20 % Criterion™ TGX Stain-Free™ Gel	Glycine

	B				8–16% Criterion™ TGX Stain-Free™ Gel	
	C				8–16% Criterion™ Tris-HCl Gel	
2	A	100 µg	60 mM DTT + 2 % CHAPS	Passive 12h	8–16% Criterion™ Tris-HCl Gel	Glycine
	B		60 mM DTT + 2 % ASB-14			
	C		5 mM TBP + 2 % CHAPS			
3	A	100 µg	5 mM TBP + 2 % CHAPS	Passive 12h	8–16% Criterion™ Tris-HCl Gel	Glycine
	B					Taurine

2.5. Western blot

Fractions enriched in synaptic proteins boiled for 5min in Laemmli buffer (62.5mM Tris/HCl, 10% glycerol, 2% SDS, 5% ß-mercaptoethanol, 0.02% bromophenol blue, pH 6.8) were resolved by SDS-PAGE. Proteins were separated on TGX Stain-Free 10% polyacrylamide gels (Biorad). Stain-Free technology contains a proprietary trihalo compound which reacts with proteins, rendering them detectable with UV exposures. Stain-Free imaging was performed using ChemiDoc MP Imager and Image Lab 4 software (Biorad) with a 2.5min stain activation time, and total protein images were therefore obtained. Proteins were then transferred to 0.2µm nitrocellulose sheet (Trans-Blot® Turbo™ RTA Midi Nitrocellulose Transfer Kit, #1704271, Biorad) using Trans-Blot Turbo Transfer System (Biorad). The quality of transfer was controlled by imaging membranes using Stain-Free technology. Membranes were then washed in TBST (15mM Tris/HCl, pH 7.6; 140mM NaCl; 0.05% Tween-20) and blocked in 5% non-fat dry milk or BSA in TBST. Membranes were then blotted in blocking solution overnight at 4°C with primary antibodies (CaMKII, 1:10000, #3357; PSD-95, 1:2500, #2507; Synaptophysin, 1:2000, #4329; Cell Signaling Technology, alpha Tubulin, 1:20000, #236-10501, Invitrogen). After 3 × 10min washes in TBST, membranes were probed with specific secondary antibodies (1:5000, Anti-rabbit IgG, HRP-linked Antibody, #7074, or Anti-mouse IgG, HRP-linked Antibody, #7076, Cell Signaling Technology) in blocking solution for 2h at room temperature, and finally extensively washed in TBST. All experimental procedures, such as blocking solutions as well as dilutions of primary and secondary antibodies were optimized for each antibody. Chemiluminescence detection was carried out using ECL Clarity (Clarity™ Western ECL Substrate, Biorad), and image capture were done with ChemiDoc MP using Image Lab 4 software.

2.6. Staining and labelling of O-GlcNAcome, phosphoproteome and whole proteome

O-GlcNAcylated proteins enzymatic labelling: O-GlcNAc residues of synapse-associated proteins were fluorescently labelled using Click Chemistry according to supplier's recommendations (Click-iT™ O-GlcNAc Enzymatic Labeling System, Molecular Probes). Coupling was done using the Alexa Fluor® 488 (Molecular Probes), with excitation and emission wavelengths of 490 and 520nm respectively.

Labelling: 100µg of protein were desalted and delipidated by chloroform/methanol/water precipitation. Protein pellet was resuspended in 1% SDS, 20mM HEPES, pH 7.9 and then heated for

10min at 90°C. After the sample cooled, the labelling buffer (2.5X in a solution containing 125mM NaCl, 50mM HEPES, 5% NP-40, pH 7.9), MnCl$_2$ (100mM), UDP-GalNAz and Gal-T1 (Y289L) were added to the sample; incubation occurred under gentle agitation for 24h at 4°C.

Coupling: azido-labelled sample was desalted by chloroform/methanol/water precipitation and the pellet was then resolubilised in 50mM Tris-HCl, pH 8.0, 1% SDS and heated at 70°C a few minutes. Click-It Reaction buffer, added with copper sulphate and two additives (one of them containing Alexa Fluor® 488 alkyne, Molecular Probes) were added to azido-labelled proteins and incubated under rotation end-over-end for 20min in dark at room temperature. The sample was finally precipitated (chloroform/methanol/water precipitation) and then resuspended in the solubilisation buffer to carry out 2D-electrophoresis as previously described.

Phosphoproteome staining: Two phosphoproteins staining have been tested: ProQ Diamond (Invitrogen) and Phospho-Tag (Applied Bio-Probes), two fluorescent dyes (excitation and emission wavelengths of 555 and 580nm, respectively); all staining steps were carried out in the dark. After fixation, gels were washed 6 x 20min with pure water. Gels were incubated with slow stirring in non-diluted ProQ Diamond or Phospho-Tag solution for 90min. Subsequent to staining, gels were destained by rinsing with stirring using a destaining solution (50mM sodium acetate pH 4.0, 20% 1, 2-propanediol for 3 x 1h, or Phospho-Tag bleaching solution (Applied Bio-Probes) 3 x 30min, for ProQ Diamond or Phospho-Tag staining, respectively. Gels were finally washed 2 x 10min with pure water.

Whole proteome staining or labelling: Different protocols based on protein staining or fluorescent labelling have been tested to detect with higher resolution and better sensitivity the whole proteome. In addition, these protocols should not interfere with other staining and labelling.

T-Red 310 labelling: The proteins were fluorescently labelled using T-Red 310 dye (T-Red 310 Protein Labeling Kit, NHDyeAGNOSTICS), according to supplier's recommendations. T-Red 310 (excitation and emission wavelengths of 650 and 665nm, respectively) was diluted in 4µl of T-Dye solvent. One hundred µg of synapse-associated proteins sample was then added to the mixture, and incubation was performed for 30min on ice.

Stain-Free technology: After UV activation, proteins in gel emit a fluorescent signal immediately detectable by imager, which makes it possible to reveal the whole protein profile of each sample which any staining prior to detection ("Stain-Free" technology, Biorad).

SYPRORuby staining: Since SYPRORuby (Invitrogen) is a fluorescent dye (excitation and emission wavelengths of 280 and 610nm, respectively), all the steps were done in the dark. Gels were incubated in SYPRO Ruby overnight. After that, gels were washed for 10min with pure water and then with a destaining solution (10% methanol, 7% acetic acid), followed by 2 x 10min washes with pure water.

Silver nitrate staining: After fixation, gel was sensitized 1min in a 0.02% sodium thiosulfate solution and placed in staining solution (0.2% silver nitrate, 37% formaldehyde) for 30-45min. Gel was then incubated in developing solution (2.5% sodium carbonate, 10% sodium thiosulfate, 37% formaldehyde) so that the proteins appear. Once the appropriate level of staining achieved, gel was placed in the "stop" solution (4% Tris-base, 2% acetic acid).

Protein visualization: Once electrophoresis achieved, 2-DE gels were rinsed in ultrapure water to remove the excess of SDS. Protein visualization sequence depends on the different staining and labelling of the three proteomes. In all cases, gels were immediately scanned using the Chemidoc MP imager and Image Lab™ software (Biorad) to detect the O-GlcNAcome (through Alexa Fluor® 488 labelling). Gels were also directly scanned if T-Red 310 labelling or Stain-Free staining have been used

for the whole proteome. The next day, following gel fixation, gels were scanned after phosphoproteome staining, and were lastly visualized the third day after whole proteome staining (for SYPRORuby or Silver Nitrate staining). Detection of fluorophores was done with blue, green, or red epi-illumination. Exposure times were chosen to gain the higher signal/background ratio without a signal saturation.

2.7. SameSpot analysis

The SameSpot analysis permitted the comparison of proteome profiles gained from sequential detection of O-GlcNAcome, phosphoproteome and whole proteome, and so to define proteins that were O-GlcNAcylated and/or phosphorylated. Expression of O-GlcNAcylated, phosphorylated and whole protein spots was analysed by SameSpot Nonlinear software (TotalLab) and was calculated as a normalized volume using spot volume and surrounding gel background.

2.8. Colloidal blue staining

Excision of spots were directly performed after colloidal blue staining. Briefly, gels were fixed in 50% ethanol and 2% phosphoric acid overnight at room temperature, and then washed 1h in 2% phosphoric acid. They were incubated in a solution of 15% ammonium sulfate, 2% phosphoric acid, 17% ethanol for 20min, and finally in the same buffer containing 0.1% Coomassie Brillant Blue G-250 (SigmaAldrich). After 3 days of staining, gels were washed in water, image captures were done with ChemiDoc MP and Image Lab software.

2.9. In-gel digestion and MALDI-TOF/TOF MS analysis

Protein identification was performed using a Proteineer workflow from Brucker Daltonics (Bremen, Germany). Colloidal Coomassie blue-stained spots were excised from preparative 2D gels. In-gel digestion and sample preparation for MALDI-TOF/TOF analysis were performed. After "in gel" trypsin digestion, peptides were extracted by the addition of 50µl of 25mM NH_4HCO_3, gel pieces were shaken for 15min, and the supernatant was collected. Two successive extractions were performed with 45% ACN/0.1% TFA for 15min. The last extraction was realized with 95% ACN/0.1% TFA for 15min. Extracts were pooled, dried in a vacuum centrifuge, and stored at -20°C until analysis. The MALDI target plate (AnchorChip, Brucker Daltonics) was covered with a cyanohydroxycinnamic acid (CHCA) matrix (0.3 mg/ml in acetone:ethanol, 3:6 v/v). Extracted peptides in 0.1% TFA were applied directly onto the CHCA matrix thin layer. The molecular mass measurements were performed in automatic mode. The MS (reflectron mode) and MS/MS (lift mode) measurements were performed off-line in automatic mode on an Ultraflex™ II TOF/TOF mass spectrometer (Bruker Daltonics) running FlexControl™ 3.3 software (Bruker Daltonics). External calibration over the 1000-3500 mass range was performed using the $[M+H]^+$ mono-isotopic ions from bradykinin 1-7, angiotensin I, angiotensin II, substance P, bombesin and adrenocorticotropic hormone (clips 1–17 and clips 18–39) from a peptide calibration standard kit (Bruker Daltonics). Briefly, each MS spectrum was acquired by accumulating data from 500 laser shots with a 25kV accelerating voltage, a 26.3kV reflector voltage and a 160ns pulsed ion extraction. Peptide fragmentation was driven by ProteinScape 2.1 (Bruker Daltonics), according to the following parameters: signal-to-noise ratio >15, more than 3 MS/MS per spot if the MS signal was available, 0.15Da of MS tolerance for peak merge and the elimination of peaks that appeared in over 35% of the fractions. Precursor ions were accelerated to 8kV and selected in a timed ion gate. Metastable ions generated by laser-induced decomposition were further accelerated by 19kV in the lift cell and their masses were measured in reflectron mode. For precursor and daughter ions, each MS/MS spectrum was produced by accumulating data from 200 and 1000 laser shots. Peak lists were generated from MS and MS/MS spectra using Flexanalysis™ 3.3 software

(Bruker Daltonics). Proteins were identified on the basis of peptide fragmentation fingerprints, according to published guidelines. Database searches with Mascot 2.3.02 (Matrix Science Ltd, London, UK) were performed in the UnitProt database via ProteinScape 2.1 (Bruker Daltonics). Taxonomy was restricted to Rodentia; a mass tolerance of 75ppm and 1 missing cleavage site for PMF and an MS/MS tolerance of 0.5Da and 1 missing cleavage site for MS/MS searching were allowed. Carbamidomethylation of cysteine and oxidation of methionine residues were considered as fixed and variable modifications, respectively. The relevance of protein identities was judged according to the probability-based Molecular Weight Search score MOWSE (calculated with $p < 0.05$).

3. Results and Discussion

3.1. Enrichment in synaptic proteins

Our objective was to obtain an enrichment of synaptic subproteome of rat sensorimotor cortex. For this purpose, a protocol consisting to successive centrifugations at different sucrose concentration (Fig. 1A), described by Kamat et al. (Kamat et al., 2014), was used. We worked on right and left sensorimotor cortex (total mass ~20mg). The aim was to keep the inter-individual heterogeneity and to avoid the pooling of biological samples.

The different centrifugation steps led to pellet/supernatant recovery, and for the isolation of crude synaptosomes-enriched P2 pellet. Our protocol was not optimized to obtain the pure synaptosomal fraction but rather to get fraction enriched in synaptic proteins, which is contaminated by neuronal, mitochondrial and glial membranes. The enrichment in synaptic proteins was confirmed by western blot analysis on initial sensorimotor cortex homogenate (total extract), light membranes and soluble enzymes fraction (S2) and synaptosomes-enriched pellet (P2). Protein profiles differed between S2 and P2 fractions (Fig. 1B, top). Enrichment of the synaptic markers (PSD-95, CaMKII and to a lesser extent synaptophysin) was observed in synaptosomes-enriched pellet P2 relative to total extract or S2 fraction, indicating successfulness of synaptic and associated proteins enrichment. Conversely, a decrease in α-tubulin, a marker of the cytoskeleton, was observed in P2 compared to S2 and total extract (Fig. 1B, bottom).

This protocol can be followed by a sucrose/percoll gradient step to obtain a pure synaptosomal fraction (Dunkley et al., 2008; Tenreiro et al., 2017).
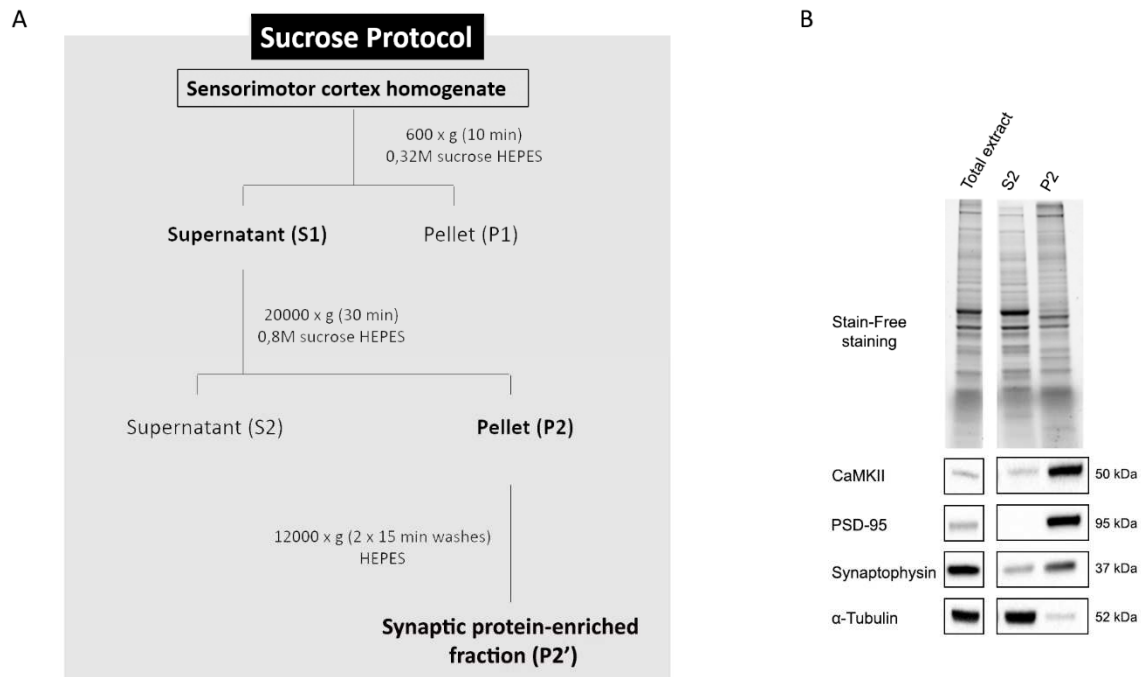
Fig. 1: Synaptic proteins enrichment in a small sensorimotor cortex sample. (A) Method is represented by the step-by-step synapse protein preparation from sensorimotor cortex and isolation of synapse protein by differential centrifugation (Awel MF-20R model, AMF20-24 rotor) with different concentrations of sucrose HEPES buffer. (B) Equal protein (10 μg) from fractions, including initial homogenate (total extract), crude synaptosomes-enriched fraction (P2), and the soluble enzymes and light membranes fraction (S2) from a fractionation of sensorimotor cortex of rat, was analyzed by western blotting for either CaMKII, PSD-95, synaptophysin, and α-tubulin. Stain-Free staining reveals the total protein profile of each fraction.

3.2. Optimization of synapse-associated proteins 2-DE

Isoelectrofocalisation was carried out on pH 3-11 nonlinear (NL) strips in order to study a large scale of proteins. Moreover, nonlinear strips produced a greater resolution in central region of gels. Since protein amount of synapse-associated proteins isolated from sensorimotor cortex tissues was low (about 3μg/μl), we used 11cm-strips to gain in protein separation without requiring higher protein quantity (see Table S1, Fig. S1, supplementary data).

To improve quality of the second electrophoretic separation, we compared different acrylamide gradients (4-20% or 8-16%) (Table 1 – Protocol #1). As shown on figure 2, majority of the spots corresponding to synapse-associated proteins were packed between 75 and 25kDa, and several spots present a molecular weight inferior to 20kDa. Thus, with a gradient of 4-20% acrylamide, upper part of the gel was uninformative since no spots were detected. In the lower part, all spots were distributed in a denser region (Fig. 2A). In contrast, with a gradient of 8-16% acrylamide, all the spots were distributed along the gel with a good detection for spots between 20 and 100kDa (Fig. 2B and C). We also assessed two gel compositions: many diffuse protein spots were observed in Tris-glycine (TGX) gel (Fig. 2B) compared to Tris-HCl gel (Fig. 2C). Based on these observations, Tris-HCl gels with an 8-16% gradient was most suitable for the separation of proteins.
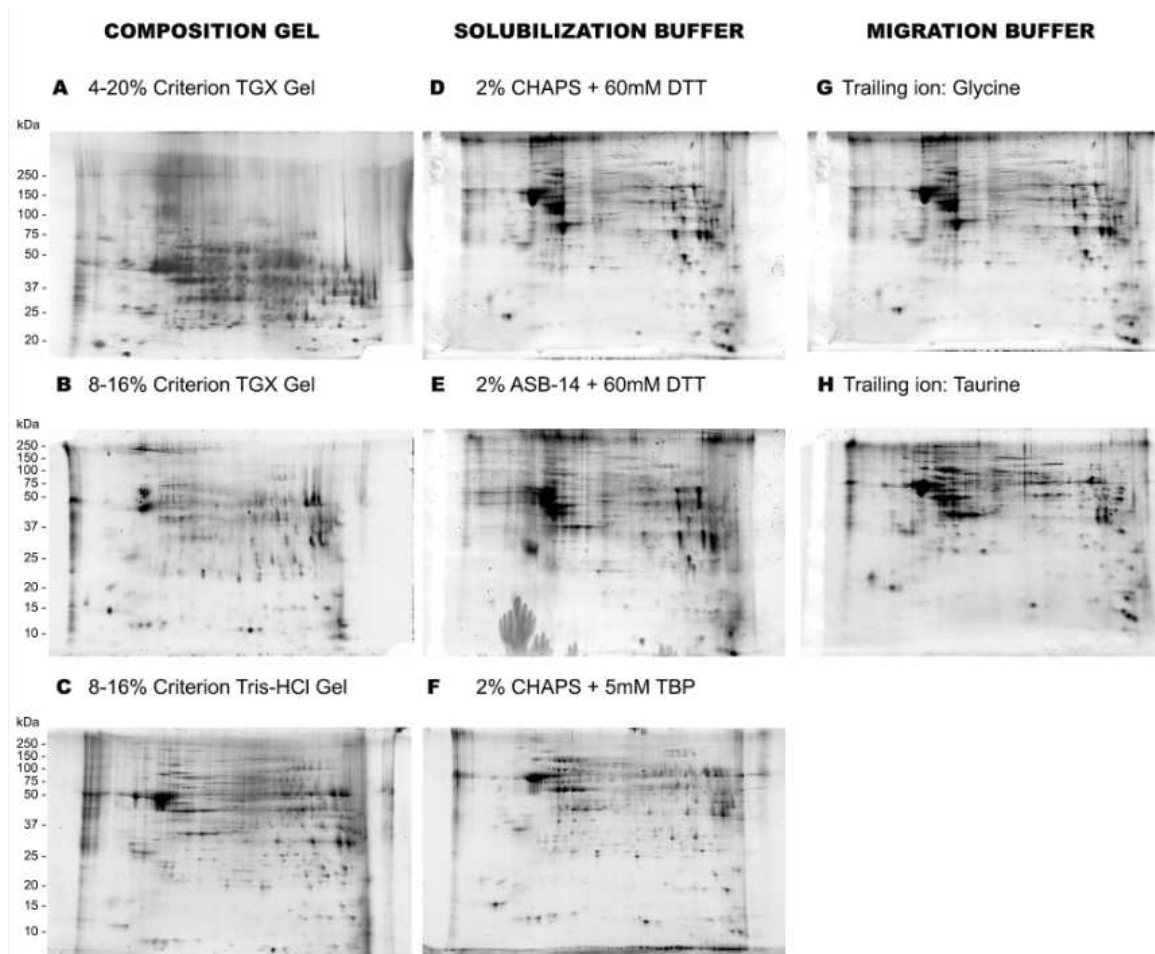
9

COMPOSITION GEL

A 4-20% Criterion TGX Gel

B 8-16% Criterion TGX Gel

C 8-16% Criterion Tris-HCl Gel

SOLUBILIZATION BUFFER

D 2% CHAPS + 60mM DTT

E 2% ASB-14 + 60mM DTT

F 2% CHAPS + 5mM TBP

MIGRATION BUFFER

G Trailing ion: Glycine

H Trailing ion: Taurine

Fig. 2. Protocols tested for IEF and SDS-PAGE optimization of synapse-associated proteins sample. The first dimension is carried out on strips of 11cm, over a pH range of 3-11 NL. Different reticulation and composition of the gel, solubilisation buffer and migration buffer have been tested according to protocols #1, #2 and #3 described in Table 1.

Using different reducing agents and detergents, we attempted to determine optimal solubilisation buffer for synaptic protein-enriched fraction (Protocol #2). All samples of proteins were solubilized in a buffer composed of urea and thiourea mix added with a reducing agent (DTT or TBP) and a zwitterionic detergent (CHAPS or ASB-14). In comparison with DTT/CHAPS mixing (Fig. 2D), combination of DTT/ASB-14 has shown a very poor separation and very low resolution of spots (Fig. 2E); in particular, several horizontal streaks were observed, suggesting that spots were poorly resolved according to their isoelectric point. ASB-14 seems to be ineffective for a proper solubilisation of synapse-associated proteins. This data is in agreement with the study of Carboni et al. (Carboni et al., 2002). Then, we have replaced DTT with TBP as reducing agent since it is reported to enhance protein solubility during IEF, therefore increasing resolution and recovery (Herbert et al., 1998). A better separation was observed for the gel image presented in Fig. 2F with respect to the Fig. 2D. Thus, we concluded that 5mM TBP and 2% CHAPS mixing in solubilisation buffer is the adequate sample buffer for optimal solubilisation of synapse-associated proteins. Rehydration step has also been optimized to improve focalisation of synapse-associated proteins during isolectrofocalisation (supplementary data, Table S1, Fig. S2).

Finally, to improve further quality of electrophoretic separation, we have tested different migration buffers varying by trailing ion (glycine, taurine, tricine) and pH range (pH8.3 or pH8.8) (supplementary data, Table S2, Fig. S3). In consequence, the glycine and taurine migration buffers at

pH8.3 were compared on second dimension (protocol #3). No significant difference was observed between Fig. 2G and 2H. Thus, for subsequent experiments, glycine migration buffer was used.

3.3. Optimization of whole proteome, phosphoproteome and O-GlcNAcome detection of synapse-associated proteins

Recently, an innovative method was developed in the laboratory to obtain three informations (O-GlcNAcylation, phosphorylation and total protein expression) from a single gel on cultured skeletal muscle cells (Cieniewski-Bernard et al., 2014). We attempted to optimize and improve this protocol for rat cerebral cortex synapse-associated proteins samples. A preliminary step of deglycosylation of O-GlcNAc residues revealed that synapse-associated proteins were mainly O-GlcNAcylated and non-N-glycosylated, that ensure a specific labelling of O-GlcNAcylated proteins (data not shown). Firstly, labelling efficiency of O-GlcNAc residues by Alexa Fluor® 488 on synapse-associated proteins was investigated (Fig. 3); significant fluorescence intensity of Alexa Fluor® 488 labelling was visualized for 40 or 100µg of synapse-associated proteins while very low signal was obtained for 20µg of synapse-associated proteins (Fig. 3A). In addition, this labelling was specific since no signal was observed for the negative controls, while a signal at the positive control (αB-crystallin) was noticed. The protein profile of each sample was visualized by Stain-Free technology (Fig. 3B). Alexa Fluor® 488 labelling of O-GlcNAc residues of synapse-associated proteins by Click chemistry is therefore effective on small amounts of proteins.
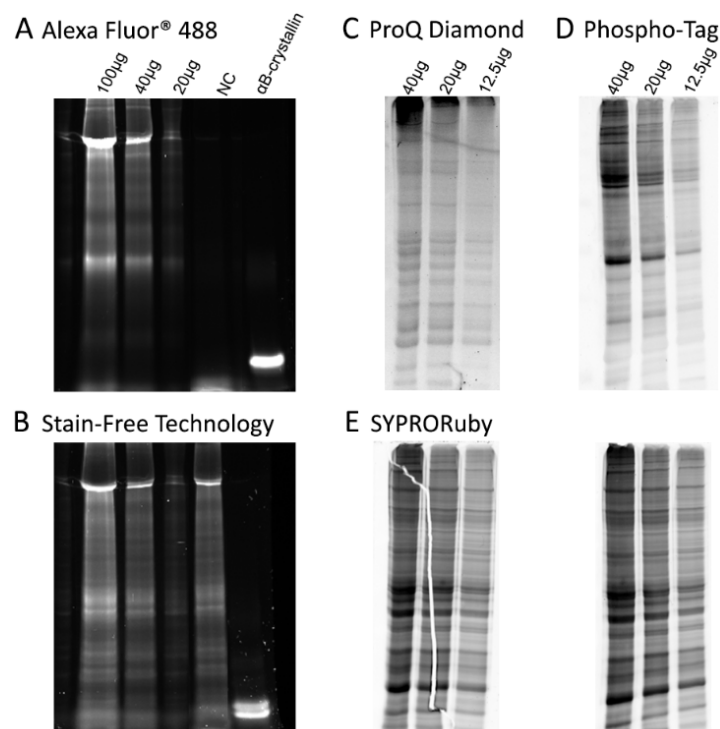

Fig. 3. Labelling of O-GlcNAc residues with Alexa Fluor® 488 and staining of phosphorylated synapse-associated proteins. (A) Labelling of O-GlcNAc residues to Alexa Fluor® 488. (B) Stain-Free staining reveals the protein profile of each sample. A quantity of proteins of 20 to 100µg was deposited for each sample. NC: Negative control; αB-crystallin: positive control. Then, two staining methods of the phosphoproteome were

compared. (C) ProQ Diamond; (D) Phospho-tag; (E) Whole proteome of each experiments stained with SYPRORuby. A quantity of proteins of 40 to 12.5µg was deposited for both conditions.

Phosphoproteins were commonly detected by ProQ Diamond staining. However, signal/noise ratio was low because background noise was high in spite of a time and a number of high washing. In addition, protein bands were poorly resolved (Fig. 3C). Subsequently, a new staining of phosphorylated proteins by Phospho-Tag was tested and was more efficient than ProQ Diamond staining (Fig. 3D). Indeed, staining was sharper and intense. The specificity of Phospho-Tag staining was tested during a dephosphorylation step by alkaline phosphatase (data not shown). In addition, background noise was low with shorter wash times. Staining of the whole proteome with SYPRORuby was quite similar whatever the staining used for phosphoproteome detection (Fig. 3E). Subsequently, the Phospho-Tag staining is preferred for phosphoprotein detection.

Different protocols of labelling or staining were carried out to detect the whole proteome (Fig. 4). Silver staining (Fig. 4A) revealed the whole proteome but provided staining with significant background noise compared to other staining protocols (Fig. 4B and C). Detection of whole proteome by Stain-Free technology (Fig. 4B) or by SYPRORuby staining (Fig. 4C) were very similar in terms of sensitivity. However, Stain-Free technology (which requires UV excitation of proteins) could interfere with other labelling, in particular with Alexa Fluor® 488 detection. Indeed, we observed a slight decrease in intensity of Alexa Fluor®488 signals when Stain-free detection was applied in first (data not shown). To permit the detection of O-GlcNAcome and whole proteome on the same day, we also labelled whole proteome with a T-Red 310 fluorophore. We observed that some spots were not detectable at whole proteome level (Fig. 4D), indicating that T-Red 310 labelling may have interfered with other stains, or was not effective enough.
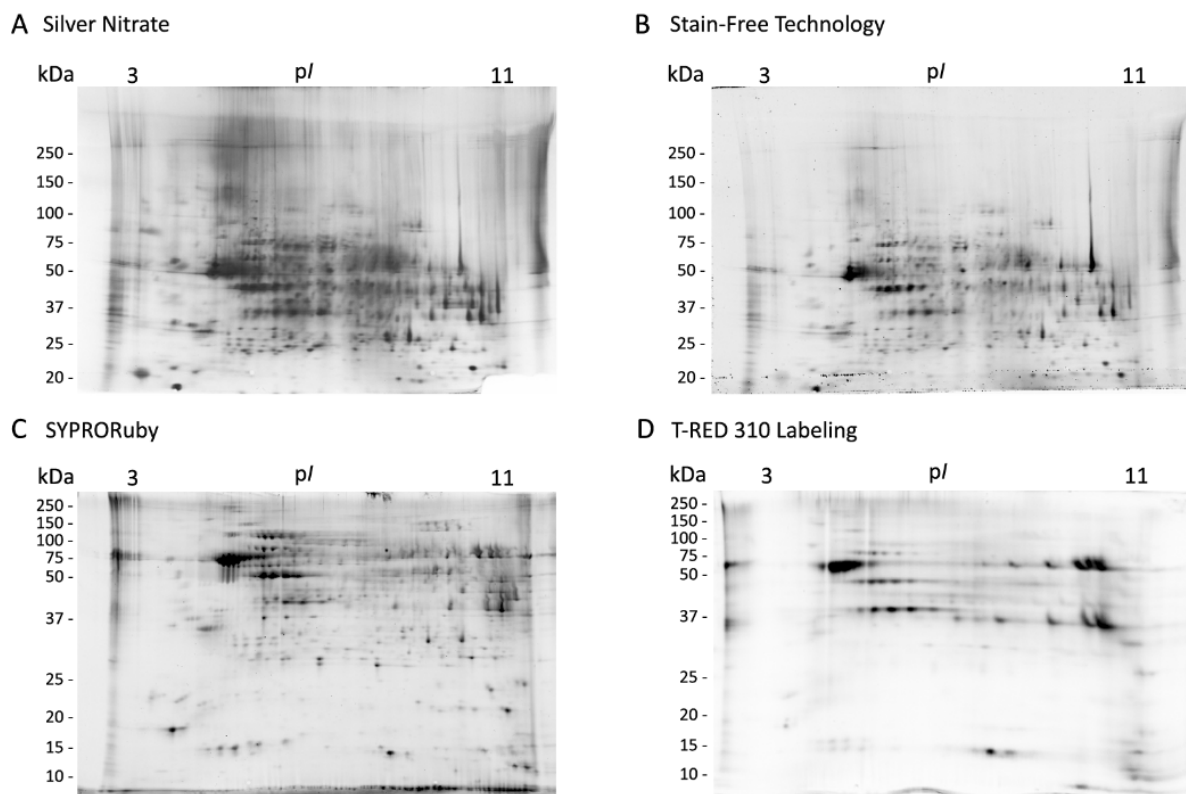

Fig. 4. Optimization of whole proteome detection. Two-dimensional electrophoresis with different staining or labelling of the total proteome. The first dimension is made on strips of 11cm, over a pH range of 3-11 NL; the

second dimension is performed on a 4-20% or 8-16% Criterion ™ TGX Stain-Free ™ or Tris-HCl gel. (A) Silver nitrate staining; (B) Stain-Free Technology; (C) Staining with SYPRORuby; (D) T-Red 310 labelling.
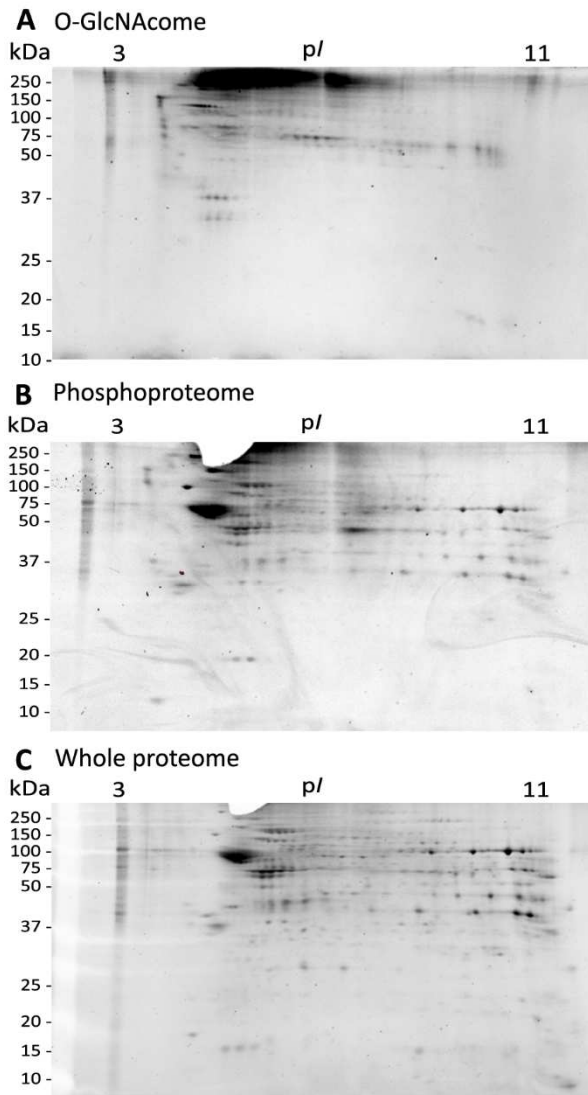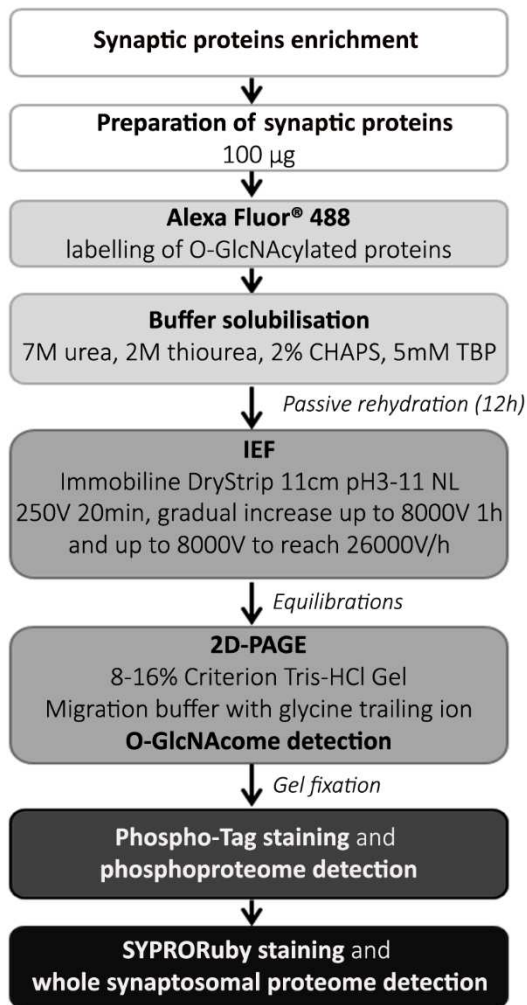
3.4. Whole proteome, phosphoproteome and O-GlcNAcome analysis of synapse-associated proteins

All these optimisations made it possible to carry out the analysis of the O-GlcNAcome (Fig. 5A), phosphoproteome (Fig. 5B) and whole proteome (Fig. 5C) of the synapse-associated proteins within the same gel. Three gels were run independently to highlight the 3 proteomes for each one. We found 408 areas corresponding to proteins spots on the reference gel image with SameSpots software. Among these areas, we highlighted spots of interest exhibiting O-GlcNAcylation and/or phosphorylation expression. More precisely, among these spots, 36% showed an O-GlcNAcylation, 24% phosphorylation, or 7% a combination (O-GlcNAcylation and/or phosphorylation). As shown in the image of the reference gel, these spots were distributed over the entire gel (Fig. 5D).

O-GlcNAcylated and/or phosphorylated spots were cut and digested with trypsin. The resulting peptides were analysed by nano-LC MS/MS. The set of identifications is presented in Table 2. Most of identified proteins are mitochondrial proteins (ex. Cytochrome c) or cytoskeleton proteins (ex. Actin-1). Others are involved in synaptic vesicle release (ex. Synaptotagmin-1).

Mitochondrial proteins. Our proteomic analysis led to the identification of mitochondrial proteins that are O-GlcNAcylated and/or phosphorylated. It has been shown that O-GlcNAcylation plays an important role in mitochondrial protein activity (Pekkurnaz et al., 2014). Thus, post-translational modifications, in particular phosphorylation and O-GlcNAcylation, may lead to changes in synaptic vesicle trafficking and activation of signalling pathways, as well as in the morphology of dendritic spines. In fact, neurons are enriched with energy-generating mitochondria (ATP, adenosine triphosphate), particularly at synapses. ATP is requisitioned for several synaptic processes: for the synaptic membrane potential, the different steps of synaptic vesicle trafficking (priming by SNARE proteins, endocytosis by clathrin coats, reloading of vesicles into neurotransmitters, transport and (Ly and Verstreken, 2006) mobilisation of synaptic vesicles from the reserve pool) and for the different signalling pathways (phosphorylation) active at the level of the synapse As a result, mitochondria play a central role in the synaptic activity.

PROTOCOL

Synaptic proteins enrichment

↓

Preparation of synaptic proteins
100 µg

↓

Alexa Fluor® 488
labelling of O-GlcNAcylated proteins

↓

Buffer solubilisation
7M urea, 2M thiourea, 2% CHAPS, 5mM TBP

↓ *Passive rehydration (12h)*

IEF
Immobiline DryStrip 11cm pH3-11 NL
250V 20min, gradual increase up to 8000V 1h
and up to 8000V to reach 26000V/h

↓ *Equilibrations*

2D-PAGE
8-16% Criterion Tris-HCl Gel
Migration buffer with glycine trailing ion
O-GlcNAcome detection

↓ *Gel fixation*

Phospho-Tag staining and
phosphoproteome detection

SYPRORuby staining and
whole synaptosomal proteome detection

A O-GlcNAcome

B Phosphoproteome

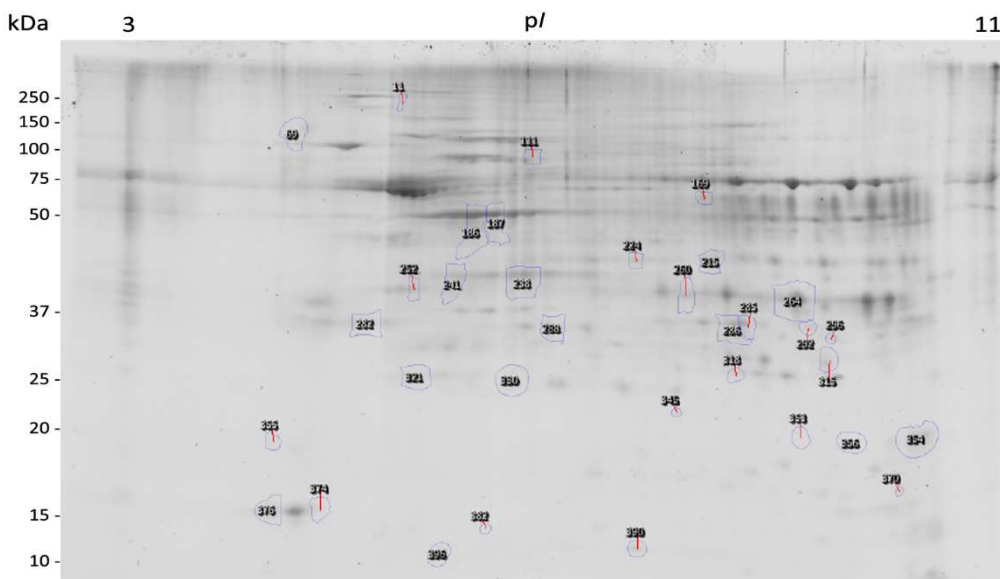**C** Whole proteome

D Whole proteome - reference gel

Fig. 5. Multiplexed detection of whole proteome, O-GlcNAcome and phosphoproteome of synapse-associated proteins. Right: Final protocol for multiplexed detection of synapse-associated proteins. Left: (A) O-GlcNAcome, labelling with Alexa Fluor® 488; (B) Phosphoproteome, staining with Phospho-tag; (C) Whole proteome, staining with SYPRORuby. (D) Whole proteome of the reference gel within SameSpots software and differential spots localization.

Table 2. List of proteins identified by mass spectrometry, within the synapse-associated proteins of the sensorimotor cortex. The identification of the proteins is detailed according to the name of the protein, its accession number (UniProtKB), its theoretical molecular mass (kDa), its sequential recovery (%), the number of peptides identified, the Mascot score, with the corresponding spot number resulting from the analysis on the SameSpots software with O-GlcNAcylation (G) and/or phosphorylation (P). The Mascot score was obtained from the Mascot database (www.matrixscience.com).

Spot N°	Accession N° (UniprotKB)	Protein name	Molecular weight (theo)	Sequence covered (%)	Number of identified peptides	Mascot score	G	P
Cytoskeleton proteins								
#11	Q4QRB4	Tubulin beta-3 chain	50.4	17.8	6	60		X
#187	P60711	Actin, cytoplasmic 1	41.7	11.2	3	208	X	
#241	P19527	Neurofilament light polypeptide	61.3	7.6	3	109	X	
Mitochondrial proteins								
#264	Q9Z2L0	Voltage-dependent anion-selective channel protein 1	30.7	25.4	4	260	X	
#315	P20788	Cytochrome b-c1 complex subunit Rieske, mitochondrial	29.4	8.8	5	70		X
#321	Q8K3J1	NADH dehydrogenase [ubiquinone] iron-sulfur protein 8, mitochondrial	24	8.5	1	46	X	
#345	P31399	ATP synthase subunit d, mitochondrial	18.8	13.0	2	88		X
#354	Q9DCJ5	NADH dehydrogenase [ubiquinone] 1 alpha subcomplex subunit 8	20	7.6	1	55	X	
#356	Q8K3J1	NADH dehydrogenase [ubiquinone] iron-sulfur protein 8, mitochondrial	24	8.5	1	52	X	
Others								
#224	P21707	Synaptotagmin-1	47.4	3.1	1	57	X	X

Cytoskeleton proteins. We identified that actin bears O-GlcNAc moieties and that β3-tubulin is phosphorylated. Actin filaments are the main components of the cytoskeleton of the synapse and are known to be modified by O-GlcNAcylation (Cieniewski-Bernard et al., 2004). Microtubules, assembled polymers of α- and β-tubulin, transiently enter the synapses, by phosphorylation/dephosphorylation process (Khan and Luduena, 1996). By recruiting regulatory proteins (actin-binding protein, actin-binding protein (ABP) protein, CaMKII) for actin and MAP (microtubule-assocative proteins, MAP2, Tau) for microtubules, synaptic activity can reshape the actin cytoskeleton and pre- and postsynaptic

microtubules (Cingolani and Goda, 2008; Conde and Caceres, 2009). Morphological changes in dendritic spines are partly achieved by reorganizing the underlying actin cytoskeleton and microtubules (Jaworski et al., 2009), thus a change in actin O-GlcNAcylation and β3-tubulin phosphorylation could therefore be correlated with changes in the size and shape of dendritic spines.

Another component of the neuron cytoskeleton, the neurofilament light chain (NF-L) that is part of the intermediate filaments family, was identified to be O-GlcNAc-modified in our proteomic analysis. Neurofilaments are believed to function primarily to provide structural support for the axon and to regulate axonal diameter (Deng et al., 2008). Neurofilaments are composed by subunits that belong, in mature neurons, to three class of proteins, the light chain, the medium chain and the heavy chain. Neurofilament proteins are extensively modified by both O-GlcNAcylation and phosphorylation: altered phosphorylation of neurofilaments may precede their accumulation in axons, while increased O-GlcNAc levels may play a protective role in the Alzheimer's disease (Deng et al., 2008).

Others. Finally, we report a substantial number of low abundant proteins identified by only one or few peptides. For the synaptic proteome, the successful identification of such proteins is of major importance since the key components of the synaptic molecular machinery responsible for neurotransmission and neuroplasticity (i.e. synaptic vesicles protein as Synaptotagmin-1) are present at very low amounts. Synaptotagmin-1 is an important calcium vesicular sensor for the spontaneous release of synaptic vesicles. Its phosphorylation by PKC is known to participate in synaptic strengthening (de Jong et al., 2016). We also show for the first time O-GlcNAcylation of this protein, essential for presynaptic function.

4. Conclusion

In this study, we determined the optimal workflow for analysis of synapse-associated proteins on small amount of brain tissue, in particular on synaptic proteins of the sensorimotor cortex, using a 2D-proteomic analysis (solubilisation buffer, gel reticulation and composition).

The first strength of this technique is to be applicable for small quantities of tissue. In fact, in the literature, proteomic analyses on synapse-associated proteins generally come from the whole brain or from samples collected to obtain a greater quantity of proteins. We did not want to pool our sensorimotor cortex samples in order to keep the interindividual differences that may exist within the same group. For this reason, fractionation with a sucrose protocol was the most satisfactory way for obtaining an adequate amount of protein. However, the main weakness of this approach is the relatively aspecific synaptosomal fractionation, and in consequence we only partially increase the chances of identifying synaptic proteins O-GlcNAcylated/phosphorylated. Indeed, a synaptosomal fractionation with sucrose or Percoll gradients and ultracentrifugation steps would have made it possible to obtain a pure synaptosomal fraction, without membrane, cellular and nuclear debris. The latter can mask differences in expression of minority synaptic proteins on 2-DE gel images. Indeed, comparing our two experimental groups, the proteins identified were mainly proteins belonging to the cytoskeleton or mitochondrials, and not predominantly synaptic proteins. In our attempt to optimize the methodological approach, we have indeed limited ourselves to around thirty differential spots whose O-GlcNAcylation and/or phosphorylation expression were observable on the gel images. However, less visible spots were perhaps more representative of synaptic proteins. Thus, it would have been interesting to select a larger number of differential spots.

The second main contribution is that, for the first time, the protocol of Click chemistry was applied on a subproteome of rat cerebral cortex synapse-associated proteins. This step and other staining

protocol optimisations allowed for a triple detection (O-GlcNAcome, phosphoproteome and whole proteome) of synapse-associated proteins on the same gel. Previous studies allowed for the identification of a set of O-GlcNAcylated or phosphorylated synapse-associated proteins (Filiou et al., 2010; Trinidad et al., 2012; Trinidad et al., 2013; Vosseller et al., 2006). However, these studies did not perform a differential analysis of proteins, or they did a differential analysis on only one proteome (Mallei et al., 2014; Tramutola et al., 2018). The advantage of the proteomic strategy optimized in our study is that once the O-GlcNAcome, the phosphoproteome and the total proteome of the synapse-associated proteins are well characterized using 2-DE gel analysis software, it is possible to detect variations in total expression, phosphorylation or O-GlcNAcylation of synapse-associated proteins between different experimental conditions (for example following a change in sensorimotor experience or in a pathological situation).

In the future, the differential analysis of O-GlcNAcome, phosphoproteome and whole proteome on a single gel will allow us to identify synaptic markers involved in activity-dependent plastic mechanisms.

5. References

Akimoto Y, Comer FI, Cole RN, Kudo A, Kawakami H, Hirano H, Hart GW. Localization of the O-GlcNAc transferase and O-GlcNAc-modified proteins in rat cerebellar cortex. Brain Research, 2003; 966: 194-205.

Carboni L, Piubelli C, Righetti PG, Jansson B, Domenici E. Proteomic analysis of rat brain tissue: comparison of protocols for two-dimensional gel electrophoresis analysis based on different solubilizing agents. Electrophoresis, 2002; 23: 4132-41.

Cieniewski-Bernard C, Bastide B, Lefebvre T, Lemoine J, Mounier Y, Michalski JC. Identification of O-linked N-acetylglucosamine proteins in rat skeletal muscle using two-dimensional gel electrophoresis and mass spectrometry. Molecular & cellular proteomics : MCP, 2004; 3: 577-85.

Cieniewski-Bernard C, Dupont E, Deracinois B, Lambert M, Bastide B. Multiplexed Detection of O-GlcNAcome, Phosphoproteome, and Whole Proteome within the Same Gel. Frontiers in endocrinology, 2014; 5: 184.

Cingolani LA, Goda Y. Actin in action: the interplay between the actin cytoskeleton and synaptic efficacy. Nature reviews. Neuroscience, 2008; 9: 344-56.

Conde C, Caceres A. Microtubule assembly, organization and dynamics in axons and dendrites. Nature reviews. Neuroscience, 2009; 10: 319-32.

de Jong AP, Meijer M, Saarloos I, Cornelisse LN, Toonen RF, Sorensen JB, Verhage M. Phosphorylation of synaptotagmin-1 controls a post-priming step in PKC-dependent presynaptic plasticity. Proceedings of the National Academy of Sciences of the United States of America, 2016; 113: 5095-100.

Deng Y, Li B, Liu F, Iqbal K, Grundke-Iqbal I, Brandt R, Gong CX. Regulation between O-GlcNAcylation and phosphorylation of neurofilament-M and their dysregulation in Alzheimer disease. FASEB journal : official publication of the Federation of American Societies for Experimental Biology, 2008; 22: 138-45.

Dunkley PR, Jarvie PE, Robinson PJ. A rapid Percoll gradient procedure for preparation of synaptosomes. Nature Protocols, 2008; 3: 1718-28.

Filiou MD, Bisle B, Reckow S, Teplytska L, Maccarrone G, Turck CW. Profiling of mouse synaptosome proteome and phosphoproteome by IEF. Electrophoresis, 2010; 31: 1294-301.

Herbert BR, Molloy MP, Gooley AA, Walsh BJ, Bryson WG, Williams KL. Improved protein solubility in two-dimensional electrophoresis using tributyl phosphine as reducing agent. Electrophoresis, 1998; 19: 845-51.

Jaworski J, Kapitein LC, Gouveia SM, Dortland BR, Wulf PS, Grigoriev I, Camera P, Spangler SA, Di Stefano P, Demmers J, Krugers H, Defilippi P, Akhmanova A, Hoogenraad CC. Dynamic microtubules regulate dendritic spine morphology and synaptic plasticity. Neuron, 2009; 61: 85-100.

Kamat PK, Kalani A, Tyagi N. Method and validation of synaptosomal preparation for isolation of synaptic membrane proteins from rat brain. MethodsX, 2014; 1: 102-7.

Khan IA, Luduena RF. Phosphorylation of beta III-tubulin. Biochemistry, 1996; 35: 3704-11.

Khidekel N, Ficarro SB, Clark PM, Bryan MC, Swaney DL, Rexach JE, Sun YE, Coon JJ, Peters EC, Hsieh-Wilson LC. Probing the dynamics of O-GlcNAc glycosylation in the brain using quantitative proteomics. Nature chemical biology, 2007; 3: 339-48.

Khidekel N, Ficarro SB, Peters EC, Hsieh-Wilson LC. Exploring the O-GlcNAc proteome: direct identification of O-GlcNAc-modified proteins from the brain. Proceedings of the National Academy of Sciences of the United States of America, 2004; 101: 13132-7.

Ly CV, Verstreken P. Mitochondria at the synapse. The Neuroscientist : a review journal bringing neurobiology, neurology and psychiatry, 2006; 12: 291-9.

Ma J, Hart GW. O-GlcNAc profiling: from proteins to proteomes. Clinical proteomics, 2014; 11: 8.

Mallei A, Failler M, Corna S, Racagni G, Mathe AA, Popoli M. Synaptoproteomic analysis of a rat gene-environment model of depression reveals involvement of energy metabolism and cellular remodeling pathways. The international journal of neuropsychopharmacology, 2014; 18.

Ogawa M, Sawaguchi S, Kamemura K, Okajima T. Intracellular and extracellular O-linked N-acetylglucosamine in the nervous system. Experimental neurology, 2015; 274: 166-74.

Pekkurnaz G, Trinidad JC, Wang X, Kong D, Schwarz TL. Glucose regulates mitochondrial motility via Milton modification by O-GlcNAc transferase. Cell, 2014; 158: 54-68.

Tenreiro P, Rebelo S, Martins F, Santos M, Coelho ED, Almeida M, Alves de Matos AP, da Cruz ESOA. Comparison of simple sucrose and percoll based methodologies for synaptosome enrichment. Anal Biochem, 2017; 517: 1-8.

Tramutola A, Sharma N, Barone E, Lanzillotta C, Castellani A, Iavarone F, Vincenzoni F, Castagnola M, Butterfield DA, Gaetani S, Cassano T, Perluigi M, Di Domenico F. Proteomic identification of altered protein O-GlcNAcylation in a triple transgenic mouse model of Alzheimer's disease. Biochimica et biophysica acta. Molecular basis of disease, 2018; 1864: 3309-21.

Trinidad JC, Barkan DT, Gulledge BF, Thalhammer A, Sali A, Schoepfer R, Burlingame AL. Global identification and characterization of both O-GlcNAcylation and phosphorylation at the murine synapse. Molecular & cellular proteomics : MCP, 2012; 11: 215-29.

Trinidad JC, Schoepfer R, Burlingame AL, Medzihradszky KF. N- and O-glycosylation in the murine synaptosome. Molecular & cellular proteomics : MCP, 2013; 12: 3474-88.
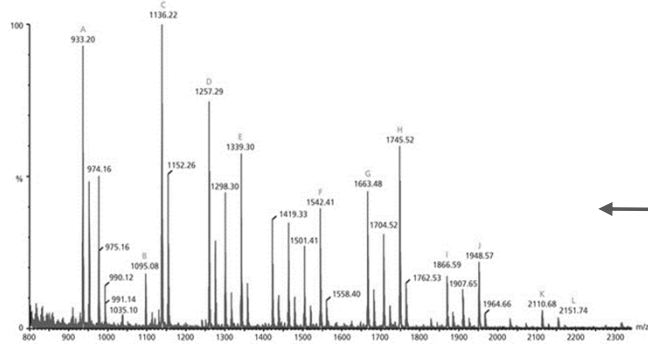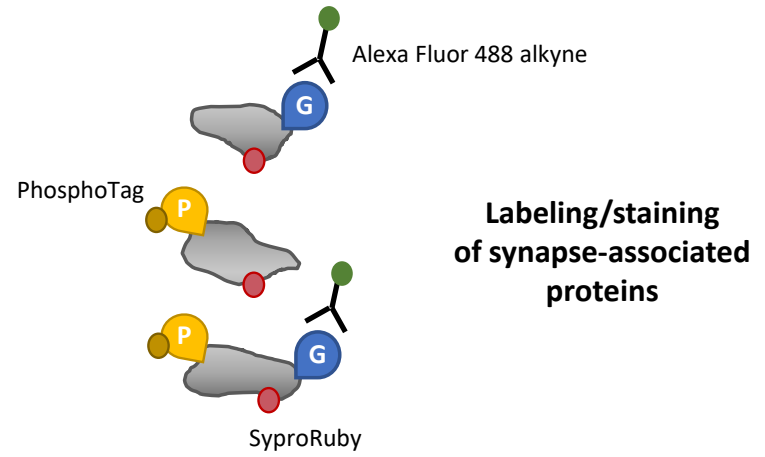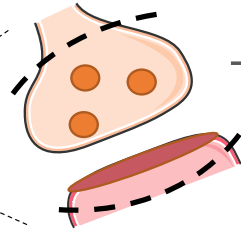
Vosseller K, Trinidad JC, Chalkley RJ, Specht CG, Thalhammer A, Lynn AJ, Snedecor JO, Guan S, Medzihradszky KF, Maltby DA, Schoepfer R, Burlingame AL. O-linked N-acetylglucosamine proteomics of postsynaptic density preparations using lectin weak affinity chromatography and mass spectrometry. Molecular & cellular proteomics : MCP, 2006; 5: 923-34.
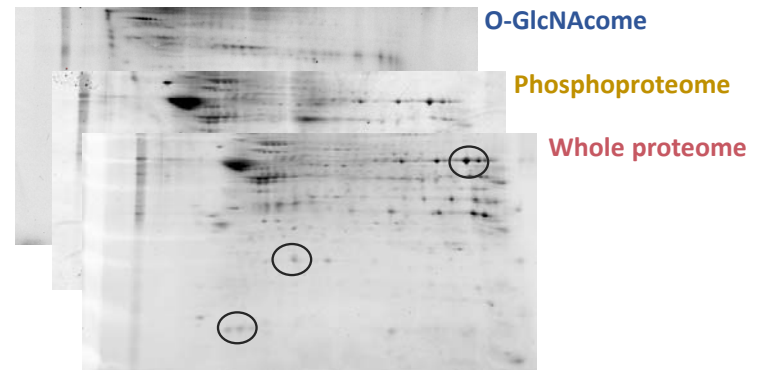
Sensorimotor cortex
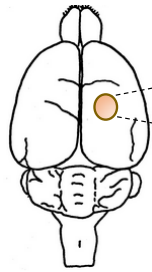
Cortical column

Synaptic proteins

Alexa Fluor 488 alkyne

PhosphoTag

G

P

SyproRuby

Labeling/staining of synapse-associated proteins

O-GlcNAcome

Phosphoproteome

Whole proteome

Bidimensional Electrophoresis

1 gel = 3 proteomes

Mass spectrometry Identification